

## Electric Field Effect in $\text{Sm}_{1-x}\text{Ca}_x\text{Ba}_2\text{Cu}_3\text{O}_y$ Bicrystal Junctions

Z. W. Dong, V. C. Matijasevic, P. Hadley, S. M. Shao, and J. E. Mooij

Applied Physics and Delft Institute of Micro-Electronics and Submicron Technology,  
Delft University of Technology, Lorentzweg 1, 2628 CJ Delft, The Netherlands

**Abstract**—A three terminal device was fabricated by depositing a thin film of Ca-doped  $\text{SmBa}_2\text{Cu}_3\text{O}_y$  on a bicrystal  $\text{SrTiO}_3$  substrate and then structuring a gate over the resulting junction. The channel shows RSJ-like Josephson junction behavior. By applying a voltage to the gate, a large electric field effect was observed. The largest field effect was observed in films where 30% of the Sm was replaced by Ca. The critical current of the junction was modulated 23% by the application of an electric field of  $5 \times 10^5$  V/cm. This electric field is about 100 times smaller than the electric field necessary for the field effects observed in homogeneous films. The sign of the field effect is consistent with that expected for a carrier-depleted grain boundary region.

### I. INTRODUCTION

It is well-established that superconductivity in cuprate thin films can be influenced by the application of electric fields [1, 2]. The largest field effects observed to date are for structures where the superconductivity is dominated by weak links [3-5]. However, as a matter of principle it has been asserted that it is also possible to induce a change in the carrier concentration on the surface of a homogeneous cuprate material. This is due to the low carrier density in the cuprates compared to conventional metal superconductors ( $n \sim 10^{21} \text{ cm}^{-3}$  cuprates and  $n \sim 10^{23} \text{ cm}^{-3}$  for metals).

Electric field effects are expected to manifest themselves when the film thickness is on the order of the electric penetration length. The electric penetration length of YBCO is estimated to be about the same as a unit cell, 1 nm. However, in the experiments using very thin films the transport properties of the films were degraded for unknown reasons. One cannot exclude the possibility that the transport was dominated by weak links in these films.

Another way to observe the field effect on a film is to use non-optimally doped material. In such a case,  $T_c$  can be increased by adding or removing holes to the  $\text{CuO}_2$  layers. Thus an increase in  $T_c$  on the surface of the film should be observed even when the film is much thicker than the electric

field penetration length. A  $\text{SmBa}_2\text{Cu}_3\text{O}_y$  (SBCO) film can be made hole-overdoped by partially substituting Ca for Sm in the film. When we apply an electric field on a 50 nm thick, 30% Ca doped film, so that  $5 \times 10^{13}$  holes/ $\text{cm}^2$  are depleted, we observe an increase in  $T_c$  by 1 K [6]. This is further evidence that a true electric field effect is possible in cuprate superconductors.

In addition, overdoped films provide another way to separate the field effects on grain boundaries from those on the films. If a negative voltage is applied to an overdoped film, more holes are induced in the film, and that causes  $J_c$  and  $T_c$  to decrease. Weak links formed at grain boundaries, however, are thought to be underdoped due to oxygen depletion. A negative gate voltage applied to a grain boundary will increase the hole density there and thus increase  $J_c$  and  $T_c$ . Therefore the two effects will have an opposite sign, in addition to the expected differences in magnitude.

Here we study the electric field effect at a single grain boundary junction. The electrodes in this experiment are the hole-overdoped superconductor Ca-SBCO. The sign of the observed electric field effect in the grain boundaries is consistent with a hole-underdoped material at the grain boundary. The required electric field for the changes which we observe in the electrical transport through the channel is 100 times smaller than that required for a homogeneous superconducting film. Similar three terminal devices employing YBCO electrodes were fabricated by Nakajima *et al.* [4] and Ivanov *et al.* [5].

The structure of the paper is the following. In section II we describe the deposition of the films and the fabrication of the field effect devices. In section III we describe the properties of the bicrystal junctions formed by depositing Ca-SBCO on bicrystal substrates. These junctions are similar to junctions formed by depositing optimally doped YBCO on bicrystal substrates, but the critical current density is lower for the Ca-SBCO. In section IV and V we discuss the field effect observed in these bicrystal junctions (JoFETs).

### II. FABRICATION OF JUNCTIONS

Films described in this paper have been made by molecular beam epitaxy (MBE) in an ozone beam. The MBE system consists of six individual elemental sources, two electron beam evaporators and four Knudsen cells, which are independently calibrated prior to deposition. The deposition is done by coevaporation in an ozone flux of  $10^{15}$  ozone molecules/ $\text{cm}^2\cdot\text{sec}$ .

Manuscript received October 17, 1994.

This work is supported by the Netherlands Program for High Temperature Superconductivity and FOM.

In this work, bicrystal Josephson junctions were made by depositing Ca-doped SBCO superconducting thin films on bicrystal SrTiO<sub>3</sub> (STO) substrates. The normal orientation of bicrystals is (100) and the tilt angle  $\theta$  in the ab-plane of the two pieces of STO facing each other is 24°. The deposition temperature used for Ca-doped SBCO is 750°C. The thickness of all the Ca-SBCO films is 50 nm. The percentage of Ca-doping was varied between 0 - 30% referring to the nominal atomic substitution of Sm. In order to protect the Ca-SBCO thin film during further processing, a 30 nm thick STO layer was deposited *in-situ* on top of Ca-SBCO at ~600°C. Afterwards, a 100 nm thick Cu layer was deposited *in-situ* at room temperature for purposes of good electrical contact to the film. Finally, all the junctions across the bicrystal boundary were defined by photolithography and Ar ion milling. The widths of junction lines used were 3, 5, 10, 15, 20, 30, and 50  $\mu\text{m}$ .

To insulate the gate electrode, either an amorphous SrTiO<sub>3</sub> (a-STO) film 200 nm thick was deposited at room temperature by MBE through a resist lift-off mask, or a polymethylmethacrylate (PMMA) layer 1  $\mu\text{m}$  thick was spun on over the grain boundary junction. Finally, an Au or Cu gate electrode 100 nm thick was deposited on top of these insulators. The size of the gate electrode was defined to be about 100  $\mu\text{m}$  long and junction line width wide. It should be noted that the Cu/STO protective layer for the bicrystal junctions was still under the insulator, acting as a floating gate (not shown in Fig. 2). The electrical contacts were made to the YBCO through the STO protective layer. The whole channel is effective for carrier modulation since the insulator gate covers the channel completely. Each sample (10 $\times$ 10 mm<sup>2</sup>) contains 14 devices.

### III. BICRYSTAL JOSEPHSON JUNCTIONS

The Ca-SBCO film is hole-overdoped and typically shows a zero resistance  $T_c$  around 40 – 80 K for different Ca-dopings [6]. Normal resistance of the junction is about 5  $\Omega\text{-}\mu\text{m}^2$  and nearly temperature independent. At 4.2 K, the critical current density is typically about 10<sup>3</sup> A/cm<sup>2</sup> and the  $I_c R_n$  product of junctions is about 0.3 mV. This  $J_c$  is 100 times smaller than YBCO bicrystal junctions with the same grain boundary angle. This makes it easier to achieve junctions without flux flow at low temperatures for 3 – 50  $\mu\text{m}$ -wide lines. The current-voltage (I-V) characteristic of our samples can be fit by the RSJ model with thermal rounding. Clear Shapiro steps were observed up to temperatures near  $T_c$ . Figure 1 shows a typical magnetic diffraction pattern and the inset shows two I-V curves taken at different magnetic fields. Although the critical current can be suppressed to zero by the application of a magnetic field, the diffraction pattern is unlike the Fraunhofer pattern. The reason for this is unclear. Similar magnetic diffraction patterns have been reported for YBCO bicrystal junctions [7]. Here, it should be noted that we measured the junction

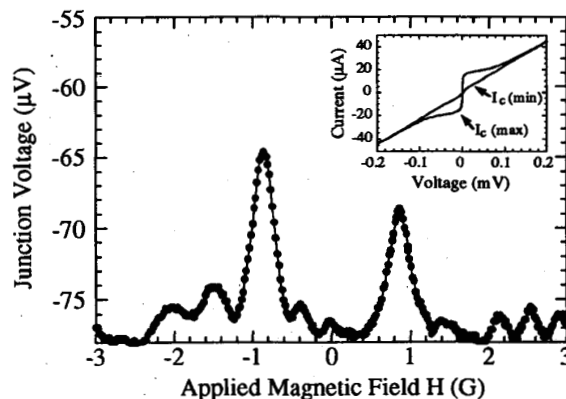


Figure 1: A typical magnetic diffraction pattern at 30 K for a 20  $\mu\text{m}$  wide Ca(30%)-SBCO bicrystal junction. The magnetic field normal to the substrate plane was applied by a solenoid above the sample. The bias current was  $-20 \mu\text{A}$ . The inset shows two I-V curves which were measured at the two magnetic fields that maximized and minimized the critical current.

voltage (instead of  $I_c$ ) dependence as a function of applied magnetic field for convenience. From the diffraction patterns, one can estimate the effective junction area to be about 2  $\mu\text{m}$  times the junction line width. This implies that, at 20 K, the effective penetration depth ( $\lambda_{\perp}$ ) in the film is at most 1  $\mu\text{m}$  and the London penetration depth,  $\lambda_L = (\lambda_{\perp} t)^{1/2}$  is no more than 220 nm. Here  $t$ , the thickness of film, is 50 nm.

### IV. JOSEPHSON JUNCTION FIELD EFFECT TRANSISTORS

Three JoFET samples have been made by using three different Ca doping levels, 0%, 10% and 30%. A schematic cross-section of the samples is shown in the inset of Fig. 2, along with a measurement circuit. The superconducting drain and source electrodes are connected by the grain boundary junction. It is generally believed that the grain boundary is oxygen deficient, so that the carrier density there is lower than that of the electrodes. Such an oxygen deficient grain boundary junction is used as a channel in our JoFETs samples. If the Josephson coupling through the grain boundary is strongly dependent on the charge carrier density, the junction behavior may be controlled by applying an electric field across the dielectric between the junction and the gate.

Gate voltage  $V_g$  was applied by a battery powered voltage source in order to keep the noise as low as possible. Our gate voltage could be varied from  $-50 \text{ V}$  to  $+50 \text{ V}$ . When a negative voltage is applied to the gate, extra holes will be added to the channel of bicrystal junctions near the Ca-SBCO/STO interface, which will increase the carrier density. In contrast, a positive gate voltage will induce hole filling and the carrier density will decrease. In this experiment, either a-STO or PMMA layer was used as the gate insulator. The

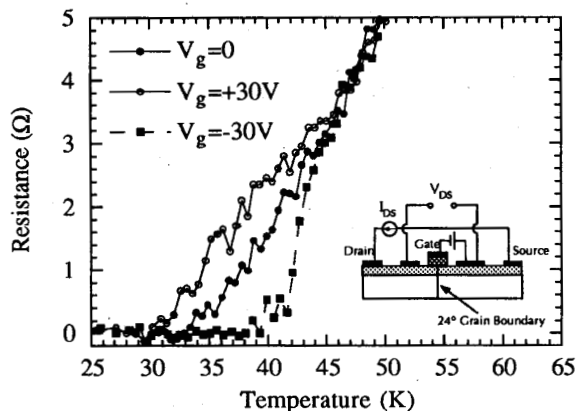


Figure 2: The resistance vs temperature for three different gate voltages. The sample is a 50 nm thick, Ca(30%)-SBCO film patterned into a 30  $\mu\text{m}$  junction. The measuring current was 1  $\mu\text{A}$ . A schematic cross-sectional view of the JoFET is shown in the inset.

breakdown field for a-STO was asymmetric. The breakdown occurs at +14 V and -2 V for a 200 nm thick a-STO at 40 K, corresponding to breakdown fields ( $E_{BD}$ ) of  $+7 \times 10^5$  V/cm and  $-1 \times 10^5$  V/cm, respectively. This is similar to the breakdown field of crystalline STO reported by Xi *et al.* and Mannhart *et al.* [1, 2]. The leakage current  $I_{leak}$  between the gate and the source is lower than 5 nA up to +12 V. This corresponds to a resistivity of  $10^9$   $\Omega\text{-cm}$  for the amorphous STO, where the gate size is  $100 \mu\text{m} \times 20 \mu\text{m}$ . This number is  $10^5$  times higher than the resistivity of a-STO reported by Ivanov *et al.* [5]. In our case, however, there is a floating gate with a crystalline STO layer under the amorphous layer. For the devices with PMMA as the dielectric layer, the breakdown voltage was above  $\pm 50$  V which was the limit of our gate voltage source. This means that the  $E_{BD}$  for the PMMA layer is greater than  $5 \times 10^5$  V/cm at low temperatures. All our experiments were carried out with  $I_{leak}$  below 1 nA which is the sensitivity of our current-meter.

In Fig. 2, the resistance  $R_{DS}$  of Ca(30%)-SBCO bicrystal junction is plotted against temperature for three different gate voltages. The measuring current was 1  $\mu\text{A}$ . The figure shows a field induced shift in zero resistance  $T_{c0}$ . The transition was broader and  $T_{c0}$  decreased by 2 K when a positive voltage of 30 V was applied. In contrast, the transition became sharper and  $T_{c0}$  increased by 6 K for a gate voltage of -30 V on the PMMA gate.

The current-voltage characteristics of many devices for undoped and Ca-doped samples were measured at different gate voltages and different temperatures. In all of these measurements, a positive gate voltage decreased both the  $I_c$  and  $T_{c0}$  while a negative gate voltage increased  $I_c$  and  $T_{c0}$ . This is consistent with an underdoped weak link at the grain boundary which dominates the transport. The undoped SBCO

sample showed a critical current modulation of +5% and -3% at 4.2 K. For the Ca(30%)-SBCO a larger modulation was achieved. At 4.2 K,  $I_c$  increased by 11% when a gate voltage of -50 V was applied and decreased by 15% when +50 V was applied. The enhancement of the critical current at 20 K is larger than it is at 4.2 K. Figure 3 shows the modulation of the I-V curves as a function of gate voltage at 20 K. At this temperature, the critical current increases 23% for a gate voltage of -30V and decreases 6% for a gate voltage of +30V. Since the hole-overdoped electrodes would cause a shift in  $I_c$  with the opposite sign, we attribute the entire modulation observed here to the electric field in the hole-underdoped grain boundary junction.

## V. DISCUSSION

Figure 4 shows the relationship between the change of the critical current as a function of the applied gate voltage for a device with a PMMA insulating layer. The critical current was maximized by adjusting the magnetic field for zero gate voltage. All other measurements were then made at this field. The voltage criterion for determining the critical current was 10  $\mu\text{V}$ .

The electric field necessary to modulate the critical current density in these bicrystal junctions is about 100 times less than the electric field necessary in a homogeneous thin film. There are two reasons for this. The first is that the carrier density in the grain boundary region is lower than in a homogeneous film. The other reason for the large electric field effects can be related to the Josephson coupling of the electrodes. It remains unclear which model most appropriately describes the Josephson coupling. However, the critical current in most models depends exponentially on the spacing

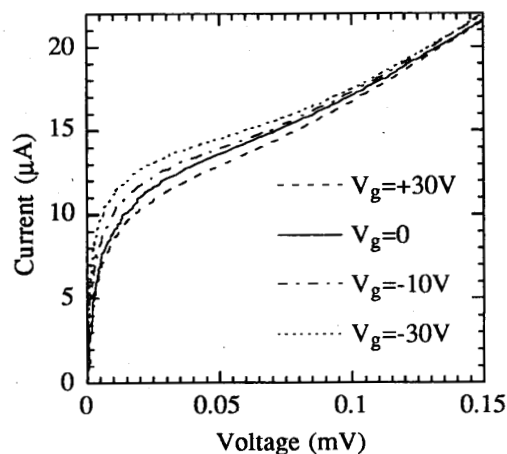


Figure 3: I-V curves for different applied gate voltages on a 15  $\mu\text{m}$  wide Ca(30%)-SBCO JoFET sample at 20 K.

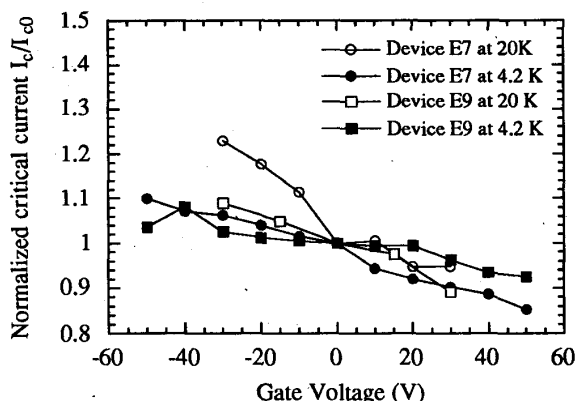


Figure 4: Normalized critical current  $I_c/I_{c0}$  vs applied gate voltage. Circles represent the  $15\ \mu\text{m}$  wide device and squares represent the  $30\ \mu\text{m}$  device. Open symbols represent data measured at 20 K and solid symbols at 4.2 K.

between the superconducting electrodes,

$$I_c \propto \exp\left(-\frac{d}{\xi}\right).$$

Here  $d$  is the spacing between the superconducting electrodes, and  $\xi$  is a parameter which determines how quickly the current decreases with increasing spacing. If the grain boundary region is appropriately modeled as a normal metal, then  $\xi$  is the normal metal coherence length. If a tunneling picture is more appropriate, then  $\xi$  is the characteristic tunneling length. Both  $d$  and  $\xi$  depend on the applied electric field. The spacing between the superconducting electrodes corresponds to the region around the grain boundary where the carrier density has been reduced to a level which, in the absence of the proximity effect, would make the material nonsuperconducting. The application of an electric field will modulate the width of this region and thus modulate the critical current. In addition to this effect, the critical current can be affected by the modulation of  $\xi$ . The magnitude of this modulation depends on the model used to describe the junction. The largest effects occur for the SNS model in the dirty limit, where  $\xi$  is proportional to  $n^{1/3}$ . Here  $n$  is the carrier density which can be modulated by an applied electric field. Since the critical current depends exponentially on the ratio  $d/\xi$ , we conclude that it is the modulation of this quantity that causes the large observed field effect.

## VI. CONCLUSIONS

We observed a large electric field effect in Ca-doped  $\text{SmBa}_2\text{Cu}_3\text{O}_y$  grain boundary junctions on  $24^\circ$  bicrystal  $\text{SrTiO}_3$  substrates. By inducing a surface carrier density of  $10^{12}$  holes/cm<sup>2</sup> we measured an increase of  $T_{c0}$  by 6 K and an increase in  $I_c$  by 23% at 20 K and 11% at 4.2 K. The sign of the field effect indicates that the critical current of the device is dominated by a hole-underdoped region. Since the

electrodes are hole-overdoped, we conclude that the electric field in the hole-underdoped grain boundary is dominating the transport. The required electric field for the field effect is about 100 times smaller than the field required in homogeneous thin films. This indicates that the electric field is modulating the Josephson coupling between the two electrodes. Such large field effects with moderate fields suggest that much greater effects can be attained by use of a better dielectric material.

## ACKNOWLEDGMENT

We would like to thank S. Bogers and H. M. Appelboom for assistance.

## REFERENCES

- [1] J. Mannhart, "Changes in the Superconducting Properties of High- $T_c$  Cuprates Produced by Applied Electric Fields," *Mod. Phys. Lett. B*, vol. 6, pp. 555-571, 1992.
- [2] X. X. Xi, C. Doughty, A. Walkenhorst, C. Kwon, Q. Li, and T. Venkatesan, "Effects of Field-Induced Hole-Density Modulation on Normal-State and Superconducting Transport in  $\text{YBa}_2\text{Cu}_3\text{O}_{7-x}$ " *Phys. Rev. Lett.*, vol. 68, pp. 1240-1243, February 1992.
- [3] J. Mannhart, J. Ströbel, J. G. Bednorz, and C. Gerber, "Large electric field effects in  $\text{YBa}_2\text{Cu}_3\text{O}_{7-d}$  films containing weak links," *Appl. Phys. Lett.*, vol. 62, pp. 630-632, February 1993.
- [4] K. Nakajima, K. Yokota, H. Myoren, J. Chen, and T. Yamashita, "Electric field effect on the artificial grain boundary of bicrystal  $\text{YBa}_2\text{Cu}_3\text{O}_{7.8}$  films," *Appl. Phys. Lett.*, vol. 63, pp. 684-686, August 1993.
- [5] Z. G. Ivanov, E. A. Stepantsov, A. Y. Tzalenchuk, R. I. Shekhter, and T. Claeson, "Field Effect Transistor Based on a Bi-crystal Grain Boundary Josephson Junction," *IEEE Trans. Appl. Supercond.*, vol. 3, pp. 2925-2928, March 1993.
- [6] V. Matijasevic, S. Bogers, N. Y. Chen, H. M. Appelboom, P. Hadley, and J. E. Mooij, "Electric Field Induced Superconductivity in an Overdoped Cuprate Superconductor," *Physica C*, vol. 235-240, pp. 2097-2098, December 1994.
- [7] N. G. Chew, S. W. Goodyear, R. G. Humphreys, J. S. Satchell, J. A. Edwards, and M. N. Keene, "Orientation control of  $\text{YBa}_2\text{Cu}_3\text{O}_7$  thin films on MgO for epitaxial junctions," *Appl. Phys. Lett.*, vol. 60, pp. 1516-1518, March 1992.